#### Research Article

Shuai Hao, Guo-ping Luo\*, Yin-sheng Chen, Yi-fan Chai, Sheng-li An, and Wei Song

# Effect of high temperature tempering on the phase composition and structure of steelmaking slag

https://doi.org/10.1515/htmp-2022-0264 received July 29, 2022; accepted December 12, 2022

Abstract: Blast furnace slag and steelmaking slag, as the main accessory products of iron and steel smelting, are piled up in large quantities due to their huge output, high treatment difficulty and low comprehensive utilization rate, which has a serious impact on the land and environment. In order to improve the comprehensive utilization of steelmaking slag, low basicity blast furnace slag was added to the existing steel slag for quenching and tempering. The influence of basicity on the chemical composition and phase precipitation of mixed slag was analyzed. In the research process, the phase composition and morphology of blast furnace slag and steel slag of Baotou Steel were analyzed using FactSage7.1 thermodynamic calculation software, ZEISS high-resolution scanning electron microscope (SEM), modern fast high-resolution Bruker energy dispersive spectrometer and AMICS-Mining automatic mineral analysis software. The results show that the mineral phase composition of blast furnace slag is mainly calcium aluminum vellow feldspar and that of steelmaking slag is mainly dicalcium silicate(C<sub>2</sub>S), magnesium-iron phase solid solution, rose pyroxene and calcium iron aluminate. When the basicity of the mixed slag is 2.0, it can effectively inhibit the formation of non-cementitious mineral anorthite and promote the formation of better cementitious mineral C2S. At the same time, it is found that the melting temperature of mixed slag decreases with the increase in Al<sub>2</sub>O<sub>3</sub> content.

**Keywords:** steelmaking slag, blast furnace slag, degree of basicity, FactSage7.1, melting temperature

## 1 Introduction

Steelmaking slag, as a subsidiary product of steelmaking, is an aggregate composed of various minerals and glassy substances [1]. Steelmaking slag shows different shapes due to different cool modes, low basicity steelmaking slag is gray, and high basicity steelmaking slag is brownish gray or off-white [2-4]. The structure of slag lump and slag shell is compact, the interface is clear, and the port is neat because of the serious vitrification of the surface layer of the quenched steelmaking slag [5]. Aging treatment [6–10] can effectively improve the stability of steelmaking slag and reduce the content of *f*-CaO in steelmaking slag. The chemical composition of steelmaking slag and Portland cement clinker is very similar to that of Portland cement clinker, and the main chemical compositions are CaO, SiO<sub>2</sub>, MgO, Fe<sub>2</sub>O<sub>3</sub>, MnO, Al<sub>2</sub>O<sub>3</sub>, and P<sub>2</sub>O<sub>5</sub> [11–13]. In addition, steelmaking slag contains a small amount of sulfide and oxide [14]. CaO is one of the main components of steelmaking slag. The quantity of calcium silicate mineral is mainly determined by SiO<sub>2</sub>, and the activity of steelmaking slag is mainly determined by the content of Al<sub>2</sub>O<sub>3</sub> [15], which mainly forms calcium aluminate or calcium aluminosilicate glass. There are three main forms of MgO [16,17], namely calcium magnesium olivine, magnesium rose pyroxene and other combined forms, RO phase solid solution, and free state magnesite, of which the combined form has good stability [18,19]. P<sub>2</sub>O<sub>5</sub> has dual properties. When its content is low, it can promote the formation of silicate minerals [20]. When the content is high, P2O5 reacts with CaO and SiO2 in the steel slag to form sodium masmitite (7CaOP<sub>2</sub>O<sub>5</sub>·2SiO<sub>2</sub> and 2C<sub>2</sub>S-C<sub>3</sub>P), which inhibits the formation of cementitious minerals C<sub>3</sub>S and C2S. The main mineral phases of steelmaking slag are C<sub>3</sub>S, C<sub>2</sub>S and RO. The mineral composition mainly depends on chemical composition and basicity. Steelmaking slag has good cementitious properties. Many researchers have done a lot of research on the structure and composition of steelmaking slag and the comprehensive utilization

High Temperature Materials and Processes 2023; 42: 20220264

<sup>\*</sup> Corresponding author: Guo-ping Luo, College of Material and Metallurgy, Inner Mongolia University of Science and Technology, Baotou 014010, China, e-mail: luoguoping3@126.com
Shuai Hao, Yin-sheng Chen, Yi-fan Chai, Sheng-li An, Wei Song: College of Material and Metallurgy, Inner Mongolia University of Science and Technology, Baotou 014010, China

of steelmaking slag in cement and concrete. Rao [21] adjusted the basicity (2.0-3.0) and Fe<sub>2</sub>O<sub>3</sub> (about 20%) of the steelmaking slag with quartz sand and coal dust. The results showed that the modified steelmaking slag f-CaO mass fraction was reduced by 39.6%, the ease of grinding index was increased by 11%, and the 7 and 28 days activity indices were increased by 3 and 4.8%, respectively. Zhang et al. [22] investigated the effect of iron tailings on the properties of high-temperature steelmaking slag. The results show that iron tailings can promote the improvement of steelmaking slag cementation, while the f-CaO content in steelmaking slag is reduced and the stability of steelmaking slag is improved. Liu et al. [23] studied the effect of blast furnace slag on the physical phase of steelmaking slag. The results showed that at 1,550°C, 10% blast furnace slag modified steelmaking slag, the mass fraction of C<sub>2</sub>S and C<sub>3</sub>S in slag increased significantly, f-CaO decreased to 1.64%, and the stability of steelmaking slag improved; in addition, coke reduced the iron in slag and improved the ease of grinding of steelmaking slag. Xiang [24] studied the preparation and foaming modification of reconstructed steelmaking slag powder with medium and high activity. The results showed that 75% converter steelmaking slag, 4% bauxite and 21% lime, fired at 1,290°C for 90 min, had the highest C<sub>2</sub>S and C<sub>4</sub>AF generation after air-cooled rapid cooling, increased water activity to 90.4%, reduced f-CaO mass fraction by 2.03%, dissipated RO phase, and increased slag ease of grinding. It was also demonstrated that the best performance of porous reconstituted steelmaking slag was achieved at a high-temperature foaming agent SiC doping of 1.6%. The activity index of the modified steelmaking slag can be increased to 98.2%, and the compressive strength of the composite cement mortar can reach 44.8 MPa. Wang et al. [25] analyzed the main components of fly ash and their role in steelmaking slag, and the results showed that  $SiO_2$  and  $Al_2O_3$  in fly ash react with f-CaO to generate stable phases, which improve the stability of steelmaking slag, while generating calcium silicate and calcium aluminate. Lei et al. [26] studied the effect of fly ash on steelmaking slag in *f*-CaO. The results show that the admixture of fly ash can reduce the f-CaO content in steelmaking slag. Li et al. [27] analyzed the effect of electric furnace slag on the properties of steelmaking slag. The results showed that the electric furnace slag can promote

the improvement of steelmaking slag coagulation. Zhang [28] studied the carbonation mechanism of zeolite-modified steelmaking slag products. The results showed that after pre-hydration curing for 1 day and carbonation for 2 h, the steelmaking slag test block with 5% zeolite (CSZ5-1 d) had the best compressive strength, and the steelmaking slag test block with 15% zeolite (CSZ15-1 d) had the best carbonation rate, which increased by 14 and 10.2% respectively compared with the pure steelmaking slag test block.

Most of the above research is to pure reagents or reducing agents to steelmaking slag reduction modification treatment, although the effect is obvious, most of the treatment methods are of high cost and cannot reach a large number of production practice applications. The blast furnace slag [29,30] is also the most solid waste resource; its basicity is around 1.0 and contains high content of Al<sub>2</sub>O<sub>3</sub>, which can be used as an effective modifier to effectively reduce the basicity of steelmaking slag, stimulate the activity of steelmaking slag and achieve the goal of "treating waste with waste." However, the experimental study on the modification of steelmaking slag by high-temperature melting of blast furnace slag is relatively few, and the phase composition and structure of steelmaking slag modified by blast furnace slag are not clear. In this article, under the premise of "comprehensive utilization of solid waste," we propose the use of water-quenched blast furnace slag to modify steelmaking slag, adjust the basicity and physical composition of steelmaking slag, eliminate the unstable factor of steelmaking slag and improve the gelation activity. It provides theoretical basis and experimental data support for the modification of steelmaking slag by blast furnace slag.

# 2 Experimental materials and research methods

#### 2.1 Experimental material

The steelmaking slag and blast furnace slag used in the test were taken from Baogang Steel, and their chemical composition was tested and analyzed using Physical and

Table 1: Main chemical composition of Baogang blast furnace slag wt%

TFe	FeO	SiO <sub>2</sub>	CaF <sub>2</sub>	S	K <sub>2</sub> O	Na <sub>2</sub> O	CaO	Mg0	MnO	Al <sub>2</sub> O <sub>3</sub>	TiO <sub>2</sub>	REO
0.36	0.69	31.58	0.94	1.27	0.35	0.46	36.72	9.28	0.44	14.79	<0.05	0.66

**Table 2:** Main chemical composition of Baogang steelmaking slag wt%

TFe	FeO	CaO	SiO <sub>2</sub>	MgO	P <sub>2</sub> O <sub>5</sub>	S	$Al_2O_3$	MnO
27.32	26.02	33.67	13.49	7.36	1.95	0.09	1.86	4.92

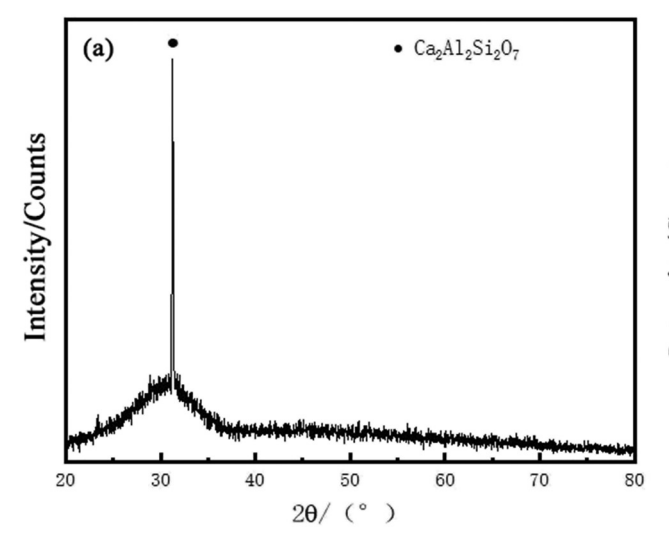
Chemical Testing Center of Baogang Rare Earth Research Institute. The results are shown in Tables 1 and 2. The content of  $SiO_2$  and  $Al_2O_3$  in the blast furnace slag is relatively high, and a small amount of  $CaF_2$  and REO are contained. The content of TFe and  $P_2O_5$  in steelmaking slag is high, and the content of  $SiO_2$  is low.

The important phases of blast furnace slag and steelmaking slag were analyzed using XRD, and the detection results are shown in Figure 1. It can be seen from Figure 1(a) and Table 1 that the main phase in the blast furnace slag is calcium aluminum melilite. According to the analysis of Table 2 and Figure 1(b), in the X-ray diffraction pattern of steelmaking slag of Baogang Steel, the diffraction angles  $2\theta$  are 32.420 and 33.067°, corresponding to the high diffraction peaks of crystal plane spacing d value of 0.276 nm and 0.271 nm. Compared with C<sub>2</sub>S standard ICSD card #86-0399, it is believed that the main mineral in the steelmaking slag of Baogang Steel is dicalcium silicate( $C_2S$ ). The diffraction angles  $2\theta$  in XRD are 36.048, 41.904, 60.844°, and the corresponding interplanar spacings d values are 0.245, 0.215, 0.152 nm; the peak surface is wider, and there are strong characteristic peaks of RO phase. Compared with the standard card (ICSD card #89-0689), it is considered that the RO phase is mainly MgO·2FeO. The diffraction angles  $2\theta$  are 33.307 and 46.512°, corresponding to low-intensity diffraction peaks

with crystal plane spacing of 0.269 and 0.195 nm. Compared with the standard card (ICSD card #70-3651), the diffraction peak is considered to be  $Ca_2(AlFe)_2O_5$ , indicating that there is a small amount of calcium ferroaluminate in the steelmaking slag. Combined with the analysis of the chemical composition of the steelmaking slag, the content of  $Al_2O_3$  in the steelmaking slag is low, and the analysis shows that the activity of the steelmaking slag is relatively low. The diffraction angles  $2\theta$  are 29.932, 35.238, and 62.358°, and the corresponding interplanar spacings d values are 0.298, 0.255, and 0.149 nm, respectively. Compared with the standard card (ICSD card #19-0629), the diffraction peak is  $Fe_3O_4$ . Other diffraction peaks have lower intensities and narrower peak areas, such as  $Ca_3MgSi_2O_8(C_3MS_2)$  and  $Ca_3SiO_5(C_3S)$ .

At the same time, the phase composition and morphology of Baogang steelmaking slag were analyzed by ZEISS high-resolution SEM, modern fast high-resolution Bruker energy spectrometer, and AMICS Mining automatic mineral analysis software. The phase composition and content of Baogang steelmaking slag are shown in Table 3.

The microstructure, content and distribution of various elements of the Baogang Steelmaking slag sample are shown in Figure 2, and its chemical composition is shown in Table 4. According to energy dispersive X-ray spectroscopy (EDS) analysis, the steelmaking slag of Baogang Steel mainly has four different color phases: dark gray phase, light gray phase, gray phase and white phase. It can be seen from Figure 2 and Table 4 that the phosphorus element in the steelmaking slag is enriched in the mineral phase C<sub>2</sub>S where point B is located, and point A is RO phase with FeO as matrix and MgO and



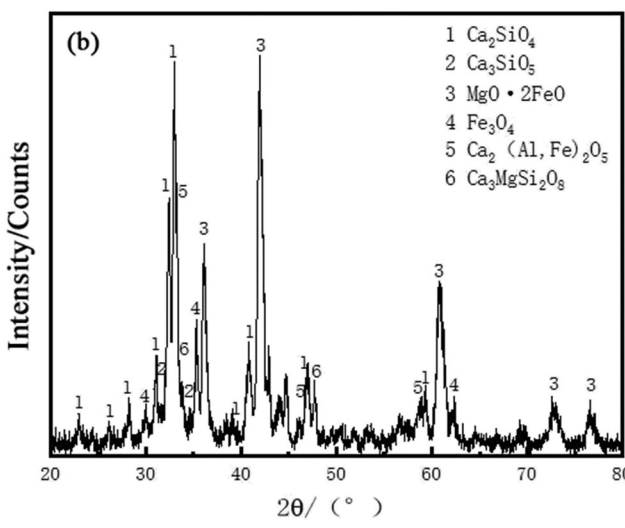


Figure 1: X-ray diffraction pattern: (a) Baogang high furnace slag; (b) Baogang steelmaking slag.

Table 3: Phase composition of Steelmaking slag of Baogang Steel wt%

Fe	Fe <sub>2</sub> O <sub>3</sub>	Ca <sub>3</sub> MgSi <sub>2</sub> O <sub>8</sub>	MgO-2FeO	Ca <sub>2</sub> SiO <sub>4</sub>	Ca <sub>2</sub> (Al,Fe) <sub>2</sub> O <sub>5</sub>	Ca <sub>2</sub> Al <sub>2</sub> SiO <sub>7</sub>	Other
14.77	1.56	24.09	20.60	23.57	7.94	0.76	6.71

MnO dissolved in solid solution. Points  $B_1$ – $B_3$  are dark gray phases, distributed in the steelmaking slag, and part of them are irregular. It is judged that they are dicalcium silicate ( $C_2S$ ) phase with a small amount of tricalcium phosphate ( $C_3(PO_4)_2$ ) dissolved. Points  $A_1$ – $A_3$  are gray oxide continuous solid solution (RO phase), containing Fe, Mg, Mn and other elements, continuously extending in dark gray phase and black phase, showing irregular shape. At point C is a gray phase yellow feldspar containing Ca, Si, O, Mg, Fe and other elements.

## 2.2 Methodology

Steelmaking slag and blast furnace slag of Baogang steel were crushed and screened repeatedly to obtain powder materials (less than 0.074 mm), drying the raw materials in an electrothermal constant -temperature blast drying oven at 105°C for 2h. The prepared raw materials were placed into a ball mill tank, mixed on the ball mill for 2 h, and then pressed into a cylinder with a diameter of  $d15 \text{ mm} \times h6 \text{ mm}$  by a tablet press under a pressure of 6 MPa. Placing into a corundum crucible and a KTF-1700-VT high-temperature vertical furnace, heating from room temperature to 1,000°C at a heating rate of 5°C·min<sup>-1</sup>, heating from 1,000 to 1,450°C with a heating system of 8°C·min<sup>-1</sup>, keeping the temperature for 1 h, and naturally cooling along with the furnace. The detection method is as follows: first, the apparent morphology of the samples after natural cooling is photographed to evaluate the selfpulverization of the samples after roasting and cooling in the furnace. Second, D8-Advanced X-ray diffractometer (Germany Brock, Germany) was used for the XRD test.

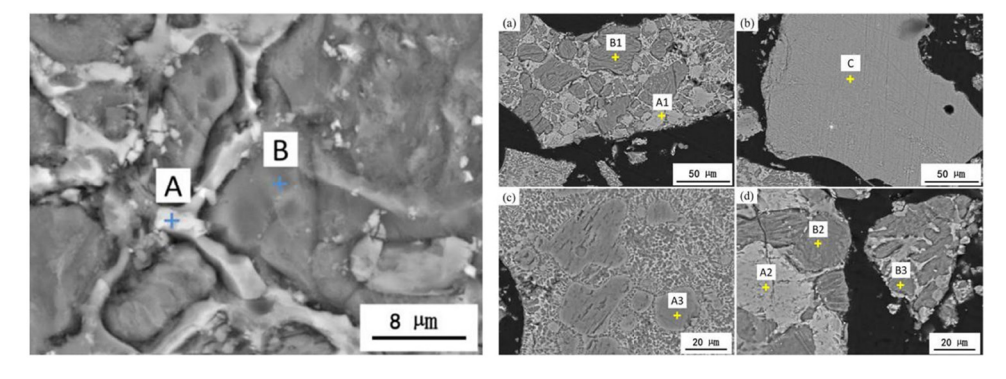


Figure 2: Morphology and EDS analysis of slag backscatter of Baogang Steel (A – MgO·2FeO; B –  $Ca_2SiO_4$ ; A1–A3 – MgO·2FeO; B1–B3 –  $Ca_2SiO_3$ ; C –  $Ca_2Al_2SiO_7$ ).

Table 4: Each phase and element content of Baogang steelmaking slag wt%

Serial number	Ca	Si	0	P	Fe	Mn	Mg	Al	Phase
A	4.31	0.30	27.52	0.08	53.49	7.67	5.00	1.26	MgO·2FeO
В	48.65	10.98	35.83	2.85	0.78	0.14	0.09	0.08	Ca <sub>2</sub> SiO <sub>4</sub>
A1	1.65	0.01	22.82	0.04	55.18	7.80	11.27	0	MgO·2FeO
A2	1.67	0.04	22.75	0	51.81	8.01	14.49	0	MgO·2FeO
A3	1.23	0.10	27.85	0.13	29.82	6.93	32.29	0	MgO-2FeO
B1	48.30	13.36	32.02	2.83	1.55	0.53	0.72	0	Ca <sub>2</sub> SiO <sub>4</sub>
B2	51.85	12.17	30.78	1.98	0.97	0.26	0.36	0.16	Ca <sub>2</sub> SiO <sub>4</sub>
В3	46.81	12.08	35.77	2.77	1.17	0.24	0.28	0.13	Ca <sub>2</sub> SiO <sub>4</sub>
C	28.48	5.27	28.21	1.03	26.84	3.85	3.17	1.26	Ca <sub>2</sub> Al <sub>2</sub> SiO <sub>7</sub>

Table 5: Ratio of mixed slag to batching

Serial number	Basicity (R)	Steelmaking slag (wt%)	Blast furnace slag (wt%)
1	1.6	53.33	46.67
2	1.8	68.19	31.81
3	2.0	79.80	20.20
4	2.2	89.17	10.86
5	2.4	96.79	3.21

Cu-k $\alpha$  target was used. Scanning type is follows: emitter–detection linkage, scanning voltage of 20 kV, and scanning current of 5 mA. The scanning range was 20–80°, and the scanning speed was  $2^{\circ}$ -min<sup>-1</sup>.

The blast furnace slag, steelmaking slag and MgO reagent of the Baogang Steel group were batched according to Table 5, and their chemical composition was shown in Table 6. With the help of Factsge7.1 thermodynamic software, the variation laws of crystallization temperature, precipitated phase and phase content of mixed slag system during the cooling process at 1,600°C cooling are simulated and calculated. The mixed slag samples were prepared, roasted and cooled. The changes of the appearance of the mixed slag samples after roasting were analyzed under the conditions of different basicities and different MgO contents. The mineral phase composition and structure of the slag samples were analyzed.

## 3 Results and analysis

## 3.1 Influence of basicity on microstructure of mixed slag

The X-ray diffraction pattern of the molten mixed slag of blast furnace slag and steelmaking slag after being roasted and cooled 1,450°C is shown in Figure 3. It can be seen from the figure that the main phase composition of the mixed slag is Ca<sub>2</sub>Al<sub>2</sub>SiO<sub>7</sub>, MgFe<sub>2</sub>O<sub>4</sub>, MgFeAlO<sub>4</sub> and

Table 6: Main chemical composition of mixed slag wt/%

Basicity (R)	FeO	CaO	SiO <sub>2</sub>	MgO	$Al_2O_3$	Fe <sub>2</sub> O <sub>3</sub>	P <sub>2</sub> O <sub>5</sub>
1.6	14.43	35.66	22.28	8.39	8.39	8.39	1.06
1.8	18.19	35.08	19.49	8.07	6.05	6.98	1.35
2.0	21.11	34.63	17.31	7.82	4.52	8.15	1.57
2.2	23.46	34.27	15.57	7.63	3.29	9.09	1.75
2.4	25.36	33.97	14.16	7.47	2.29	9.84	1.90

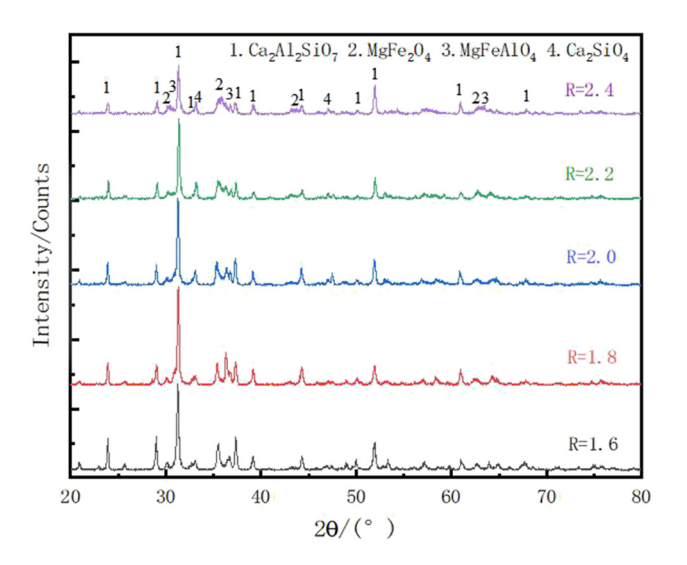


Figure 3: XRD Patterns of mixed slag with different basicities.

 $\text{Ca}_2\text{SiO}_4$ . The intensity of the diffraction peak will change after the mixed slag with different basicities is roasted and cooled. The main peak of the X-ray diffraction pattern of mixed slag (R=1.6-2.4) after roasting and cooling is non-gel phase gehlenite ( $\text{Ca}_2\text{Al}_2\text{SiO}_7$  and  $\text{C}_2\text{AS}$ ), which is a kind of stone group mineral and belongs to plagioclase. Comparing the diffraction angles of XRD patterns of five different basicities, it is found that the diffraction peak intensity of gehlenite decreases gradually with the increase of basicity.

When the basicity of mixed slag is 1.6-2.0 and  $2\theta=33.034^\circ$ , the diffraction peak intensity of  $Ca_2SiO_4$  ( $C_2S$ ) changes from weak to strong with the increase of basicity. When the basicity of mixed slag is between 2.0-2.4 and  $2\theta=33.034^\circ$ , the diffraction peak intensity of  $C_2S$  changes from strong to weak with the increase of basicity. There are a few diffraction peaks of MgFe<sub>2</sub>O<sub>4</sub> and spinel MgFeAlO<sub>4</sub> in the XRD, but the intensity of diffraction peaks does not change significantly with the change of basicity.

There are some differences between XRD mineral composition of mixed slag and thermodynamic simulation results under an equilibrium state. The reason is that the cooling conditions are different. Thermodynamic calculation can accurately calculate the cooling rate and the phase composition of the corresponding temperature equilibrium state, while the experimental study corresponds to the non-equilibrium state with furnace cooling. Comparative analysis shows that controlling the cooling rate is beneficial to the crystallization of solid solution (including spinel),  $\alpha'$ -C<sub>2</sub>S and C<sub>2</sub>SP. Natural cooling is beneficial to the phase crystallization of calcium aluminite, magnesium ferrite and spinel. Therefore, it is expected to form and precipitate more  $\alpha'$ -C<sub>2</sub>S and C<sub>2</sub>SP crystals by controlling the cooling regime.

6 — Shuai Hao *et al.* DE GRUYTER

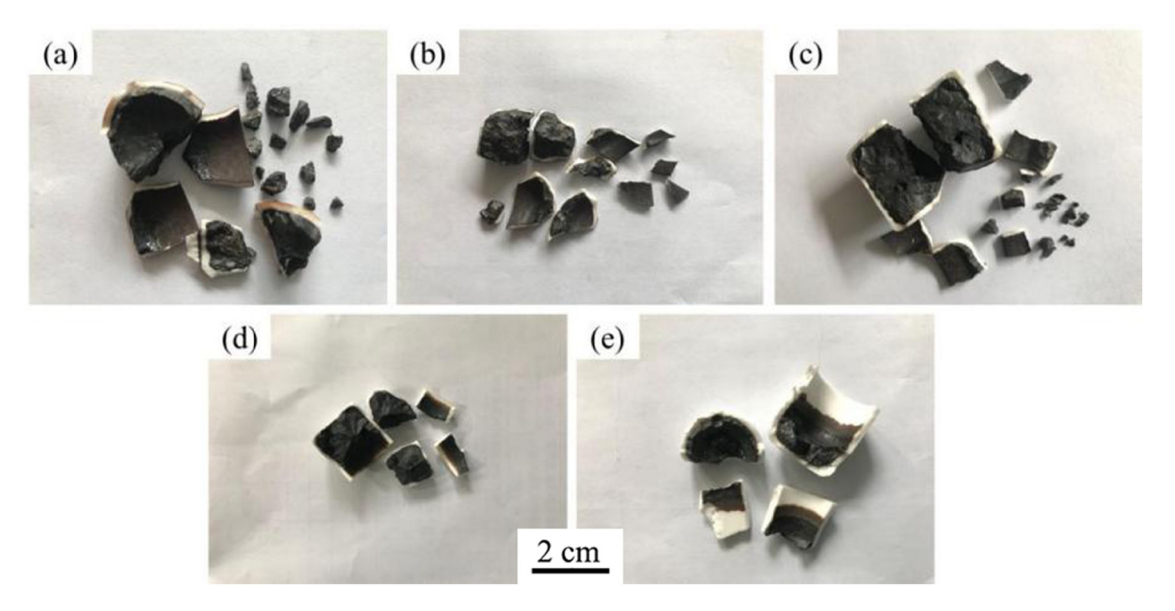


Figure 4: Roasting of mixed slag with different basicities at 1,450°C: (a) R = 1.6; (b) R = 1.8; (c) R = 2.0; (d) R = 2.2; (e) R = 2.4.

The situation of the molten mixed slag of blast furnace slag and steelmaking slag after baking and cooling in the furnace is shown in Figure 4 (the crucible is cracked after cooling). It can be seen from the figure that when the basicity is between 1.6 and 2.4, the mixed slag after high-temperature roasting is in the form of a molten block, which is bonded with the wall of the corundum crucible without pulverization.

The SEM picture of the mixed slag baking cooling sample is shown in Figure 5. The composition of each phase of the mixed residue sample was analyzed using EDS analyzer, and the detection results of element content are shown in Table 7. According to Figure 5, there are five main mineral structures in the mixed slag. The white area (point A) is MgFe<sub>2</sub>O<sub>4</sub> phase, the gray-black area (point B) is calcium-aluminite phase (C<sub>2</sub>AS), the gray area (point C) is phosphorus-rich C<sub>2</sub>S phase, and the light gray area (point D) is spinel phase and (point E) calcium ferrite phase.

The MgFe<sub>2</sub>O<sub>4</sub> phase mainly contains iron and magnesium oxides and iron manganese oxides. The main elements of gehlenite are Ca, Al, Si and O. The phosphorus-rich phase mainly exists in the form of  $Ca_7P_2Si_2O_{16}(2C_2S-C_3P)$ . In the slag,  $P_2O_5$  reacts preferentially with CaO to form  $Ca_3(PO_4)_2$ , which occurs in the  $C_2S$  phase and inhibits the crystal transformation of  $C_2S$ . With the increase of basicity of the mixed slag, the concentration of CaO and  $SiO_2$  changes, and the content of  $SiO_2$  and  $Al_2O_3$  gradually decreases, so that the production of calcium aluminite gradually decreases. Fe<sup>2+</sup>, Fe<sup>3+</sup> and  $Ca^{2+}$  produce calcium ferrite or calcium aluminate, which is gray and amorphous.

Spinel is composed of oxygen, magnesium, iron, aluminum, manganese and other elements of a mineral; its appearance is transparent color beauty and is used as a gem. In the SEM mineral phase diagram, MgFeAlO<sub>4</sub> spinel shows massive crystals and contains trace Mn elements. Compared with the mixed slag phase diagram with a basicity of 1.6–1.8, the distribution of spinel in the mixed slag phase diagram with a basicity of 2.0–2.4 is more. It is considered that the spinel in the mixed slag phase increases with the increase in basicity.

In order to further determine the distribution of elements and mineral phases in the molten mixed slag of blast furnace slag and steelmaking slag with different basicities, the mixed slag roasted samples with basicity of 1.6 and 2.0 were scanned using SEM. The results are shown in Figure 6. According to Figure 6(1), a large amount of Mg, Fe, O and Mn elements cover the white area of point A in the mineral phase diagram of mixed slag with a basicity of 1.6, and area A is considered to be MgFe<sub>2</sub>O<sub>4</sub> phase containing Mn element. A large amount of Ca, Al, Si and O elements are uniformly distributed in the gray and black area of point B, which is consistent with the element analysis result of point scan and is considered to be the Ca<sub>2</sub>Al<sub>2</sub>SiO<sub>7</sub> phase. The gray area of point C contains a large number of Ca, O, and P elements and a small amount of Si elements, which is considered a P-rich phase C<sub>2</sub>S.

Figure 6(2) shows that the light gray area of point D in the mineral phase diagram of the mixed slag with a basicity of 2.0 (lumpy crystal) contains a large amount of Mg, Fe, Al, O and trace Mn, which is considered to be MgFeAlO<sub>4</sub>, and there may be trace MnFeAlO<sub>4</sub>. The light

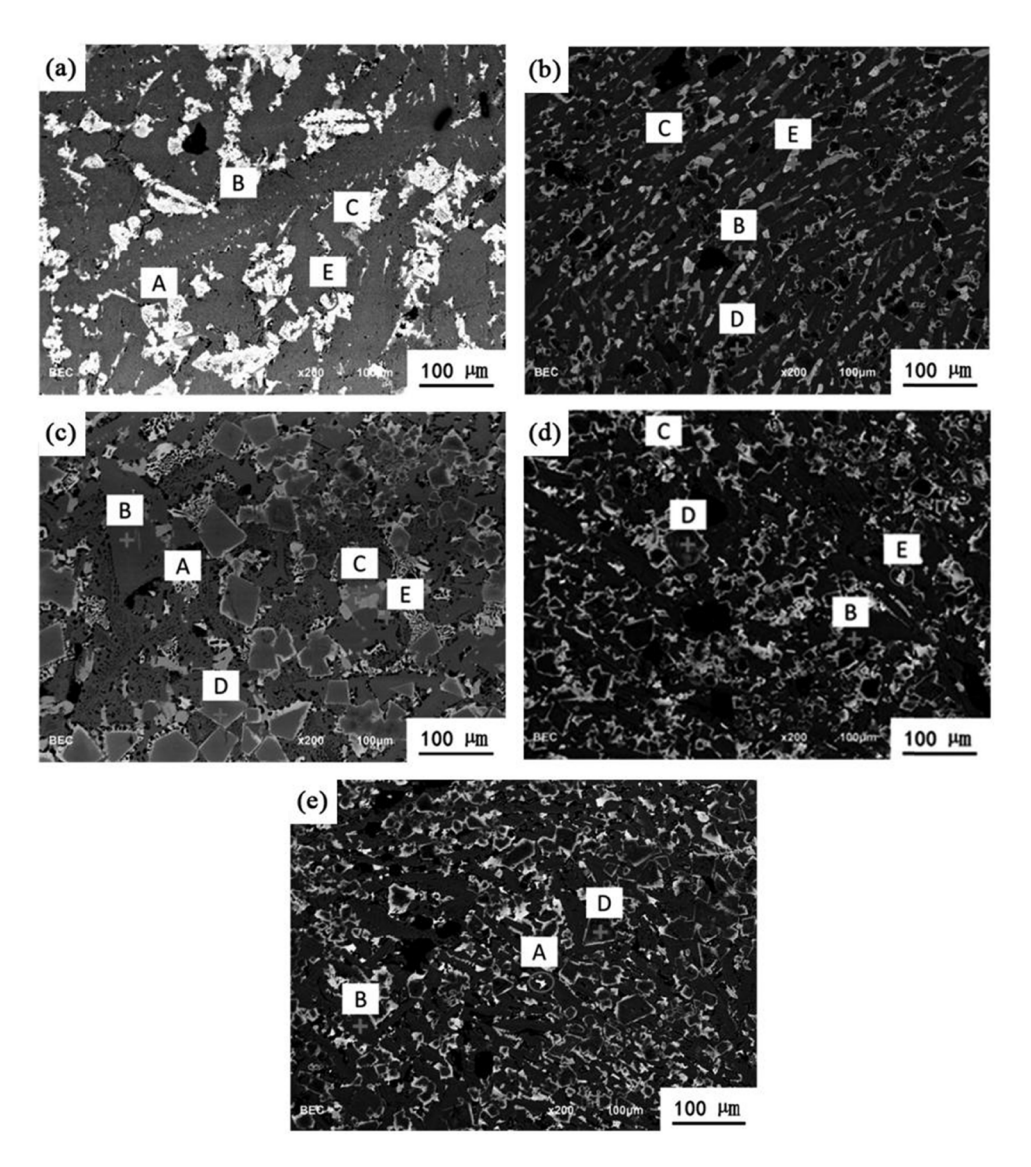


Figure 5: SEM mineral phase composition of mixed slag (A – MgFe<sub>2</sub>O<sub>4</sub>; B – Ca<sub>2</sub>Al<sub>2</sub>SiO<sub>2</sub>; C – Ca<sub>2</sub>SiO<sub>4</sub>-Ca<sub>3</sub>(PO<sub>4</sub>)<sub>2</sub>; D – MgFeAlO<sub>4</sub>; E – Ca<sub>2</sub>Fe<sub>2</sub>O<sub>5</sub>: (a) R = 1.6; (b) R = 1.8; (c) R = 2.0; (d) R = 2.2; (e) R = 2.4).

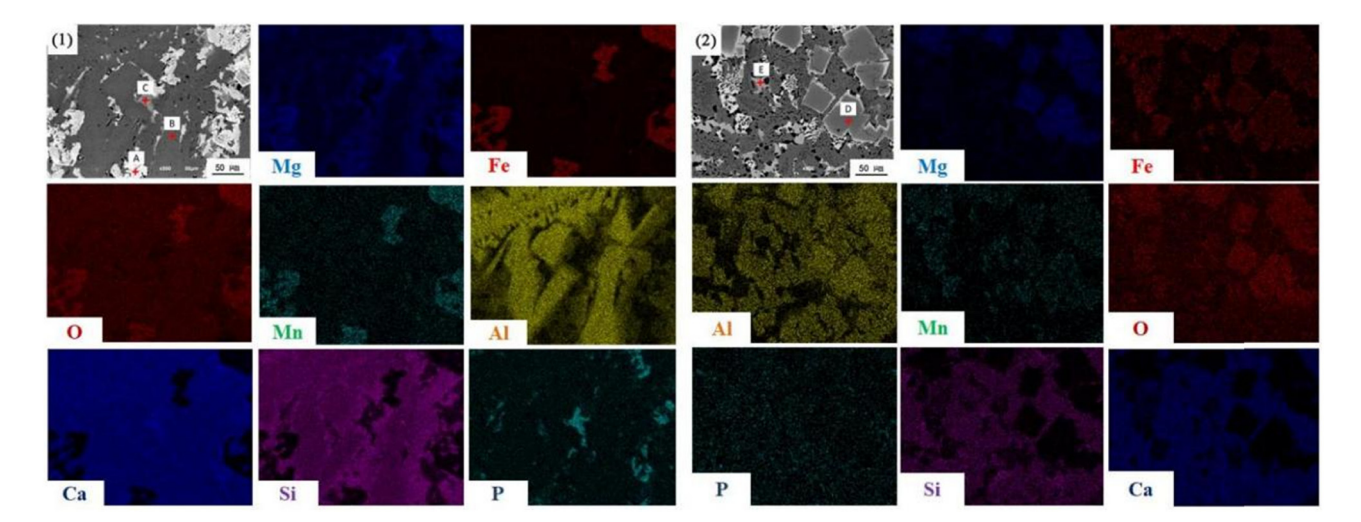
gray area of point E is mainly distributed with Ca, Fe and O elements, mixed with trace P, Mn and Mg elements. Combined with the energy spectrum data in Table 7, point E is judged to be Ca<sub>2</sub>Fe<sub>2</sub>O<sub>5</sub> phase. Therefore, it is believed that the qualitative results of phase are more accurate after XRD analysis, SEM point scanning and surface scanning analysis of the roasting samples with different basicities of blast furnace slag and steelmaking slag melting mixture.

Table 8 and Figure 7 are the results of composition and content calculated using binary method for roasted samples of molten slag and steelmaking slag with different basicities. Combined with the figure, it can be seen that with the increase of basicity from 1.6 to 2.4, the content of calcium-aluminite phase in the mixed slag decreases from 62.56 to 30.28%, the content of spinel phase increases from 4.82 to 27.13%. The content of the calcium ferrite phase increased from 9.35 to 14.63%, and the content of the magnesium ferrite phase increases from 5.29 to 5.91%. When the basicity increases from 1.6 to 2.0, the content of the dicalcium silicate phase increases from 12.59 to 13.67%. When the basicity increased from 2.0 to 2.4, the content of the dicalcium silicate phase decreased from 13.67 to 12.46%. It shows that the change of basicity of mixed slag will directly affect the content change of phase composition of mixed slag.

8 — Shuai Hao et al. DE GRUYTER

Table 7: Element content in each phase of mixed slag with different basicity wt%

Basicity (R)	Serial number	Ca	Si	0	P	Fe	Mn	Mg	Al
R = 1.6	А	2.17	1.22	24.07	0.36	52.50	11.48	5.92	1.30
	В	29.98	15.18	28.24	0.41	5.45	0.25	1.70	17.74
	С	40.25	7.95	27.17	13.55	2.12	0.68	0.91	0.94
	E	15.86	4.55	25.98	1.35	15.87	1.92	1.61	1.58
R = 1.8	В	29.98	14.03	28.10	0.21	5.43	0.62	0.65	19.16
	С	46.29	4.99	23.58	15.33	1.34	0.34	0.18	0.24
	D	0.32	0.04	28.23	0.31	25.50	3.57	15.22	23.62
	E	15.97	4.73	26.43	1.34	15.97	1.88	1.05	1.84
R = 2.0	Α	2.21	1.44	23.60	0.44	50.54	11.43	7.65	1.18
	В	28.82	13.82	31.01	0.07	8.54	0.33	1.28	15.79
	С	47.01	5.98	24.38	15.23	1.28	0.35	0.19	0.22
	D	0.32	0	28.86	0.15	26.34	3.87	15.11	23.93
	E	16.49	6.00	27.82	0.93	18.49	2.18	0.63	1.47
R = 2.2	В	29.34	13.78	29.00	0.26	7.32	0.19	0.77	18.99
	С	46.65	6.06	23.98	14.88	1.26	0.34	0.79	0.24
	D	0.33	0.08	28.05	0.41	24.76	3.76	15.72	25.16
	E	17.15	2.24	26.84	0.63	17.48	6.05	2.67	1.33
R = 2.4	Α	1.28	1.38	20.35	0.52	56.25	11.58	6.25	1.87
	В	29.88	12.22	28.73	0.40	7.06	0.23	0.17	20.35
	D	0.38	0.05	28.02	0.38	25.68	3.42	15.03	26.18



**Figure 6:** SEM scanning of mixed slag ((1) R = 1.6; (2) R = 2.0; (A) MgFe<sub>2</sub>O<sub>4</sub>; (B) Ca<sub>2</sub>Al<sub>2</sub>SiO<sub>7</sub>; (C) Ca<sub>2</sub>SiO<sub>4</sub>-Ca<sub>3</sub>(PO<sub>4</sub>)<sub>2</sub>; (D) MgFeAlO<sub>4</sub>; (E) Ca<sub>2</sub>Fe<sub>2</sub>O<sub>5</sub>).

**Table 8:** Test results of phase composition and content of mixed slag with Basicity R = 1.6-2.4 wt%

Phase (mean)	Voids	Ca <sub>2</sub> Al <sub>2</sub> SiO <sub>7</sub>	MgFeAlO <sub>4</sub>	Ca <sub>2</sub> SiO <sub>4</sub>	CaFe <sub>2</sub> O <sub>4</sub>	MgFe <sub>2</sub> O <sub>4</sub>
R=1.6	5.39	62.56	4.82	12.59	9.35	5.29
R = 1.8	7.20	57.13	8.29	12.65	9.42	5.31
R = 2.0	10.96	37.16	23.16	13.67	9.59	5.46
R = 2.2	12.72	33.85	24.28	12.71	10.80	5.64
R = 2.4	9.59	30.28	27.13	12.46	14.63	5.91

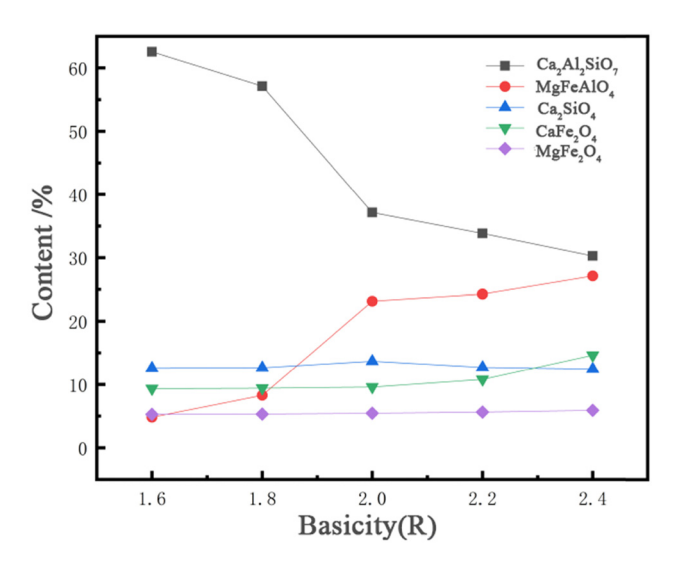


Figure 7: Composition and content of roasting mixed slag with different basicities calculated by the binary method.

## 3.2 Influence of basicity on melting property of mixed slag

The equilibrium phase composition and melting temperature of mixed slag with different basicities of liquid module in FactSage7.1 were analyzed. The specific parameter Settings are shown in Table 9.

## 3.2.1 Thermodynamic simulation of basicity on melting property of mixed slag

According to the batching ratio of mixed slags (R = 1.6-2.4) in Table 5, Factsage7.1 thermodynamic software was used to simulate the influence of different basicities on the melting temperature of mixed slags. The calculation results are shown in Table 10 and Figure 8. With the increase of basicity, the initial melting temperature shows a trend of first increasing and then decreasing. The analysis shows that the content of steelmaking slag increases with the increase in basicity. However, TFe in steelmaking slag reacts with CaO and SiO<sub>2</sub> in slag to form calcium and iron olivine (CaO·FeO·SiO<sub>2</sub> and CFS) phase.

 $\begin{tabular}{ll} \textbf{Table 10:} Liquidus temperature of mixed slag samples of variable \\ basicity series/ {\rm ^{\circ}C} \end{tabular}$ 

Basicity (R)	1.6	1.8	2.0	2.2	2.4
Solidus temp	1231.45	1233.91	1159.98	1156.12	1152.27
Liquidus	1453.98	1532.71	1583.24	1619.17	1642.33
temperature					

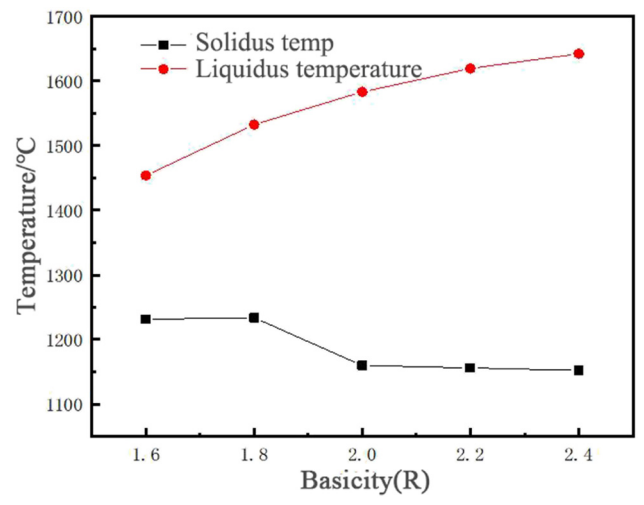


Figure 8: Melting temperature of mixed slag samples with variable basicity.

The melting point of CFS olivine is 1,205°C, so the initial melting temperature increases slightly when the basicity is 1.6–1.8. With the basicity increasing from 1.8 to 2.4, a low melting point silicate phase is formed in the mixed slag, which makes the initial melting temperature decrease continuously. From 1231.45 to 1152.27°C, while the liquidus temperature has been increasing, the melting temperature range has been increasing. The analysis shows that with the increase of basicity, a small amount of silicate with a low melting point is formed in the mixed slag, so that the melting temperature is lowered, while the content of  $Al_2O_3$  in the mixed slag is reduced, and the formation of gehlenite with low melting point is reduced, so that the liquidus temperature of the mixed slag is increased.

Table 9: FactSage7.1 parameter settings

The database	FToxid7.1, FactPS7.1
Compound type Solid solution	Monoxide FToxide-SLAGA, FToxide-SPANA, FToxide-MeO-A, FToxide-cPyrA, FToxide-oPyr, FToxide-pPyrA, FToxide-LcPy, FToxide-WOLLA, FToxide-bC <sub>2</sub> S, FToxide-aC <sub>2</sub> S, FToxide-Mel, FToxide-OlivA

Table 11: Test results of melting point of mixed slag with different basicity/°C

Basicity (R)	Softening temperature	Hemisphere temperature	Flow temperature	Soft melting range
1.6	1,316	1,318	1,332	16
1.8	1,334	1,341	1,351	17
2.0	1,344	1,362	1,368	24
2.2	1,371	>1,373	>1,373	_
2.4	>1,373	>1,373	>1,373	_

Note: melting temperature = hemispherical temperature; softening interval = flow temperature - softening temperature; liquidus temperature is the temperature at which the solid phase melts completely during the heating process, which is called the complete melting temperature of the mixed slag.

## 3.2.2 Experimental study on the melting performance of mixed slag by basicity

The CQKJ-II hemispherical melting point melting rate synthetic tester was used to study the influence of different basicities on the melting temperature of the molten mixture of blast furnace slag and steelmaking slag, and the results are shown in Table 11.

The melting temperature (softening temperature, hemispheric temperature, flow temperature and liquidus temperature) of the mixed slag varies with basicity as shown in Figure 9. It can be seen from the figure that with the increase of basicity, the softening, hemispherical, flowing and liquidus temperatures of the mixed slag increase. According to thermodynamic data analysis that: mixing slag in the process of heating up, have been dissolved equilibrium phase  $C_2AF$ ,  $\alpha'-C_2S$ , rich phosphorus phase  $C_2SP$ , melilite, magnesium rhodonite ( $Ca_3MgSi_2O_8$ ,  $C_3MS_2$ ) and solid solution (including spinel). With the increase of basicity, the addition of steelmaking slag increases, which changes the shape of the spinel solid solution in mixed

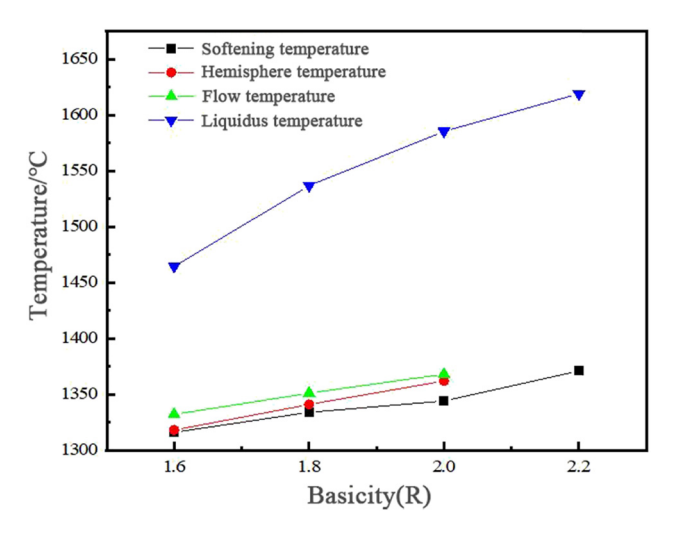


Figure 9: Melting properties of mixed slags with variable basicity.

slag, and the melting temperature of the solid solution increases from 1,400 to 1,600°C. The melting temperature of mixed slag changes with the change. Due to the limitation of experimental equipment, the highest actual temperature of the melting rate tester can only reach 1,373°C, so the specific data of melting temperature with basicity between 2.2 and 2.4 cannot be obtained.

When the basicity is between 1.6 and 2.0, with the increase of the basicity, the softening, hemisphere, flow and liquidus temperature of the mixed slag are greatly increased, the softening and melting temperature range is increased, the hemisphere temperature is increased from 1,318 to 1,362°C, and the liquidus temperature increases from 1453.98 to 1583.24°C, namely, the hemisphere temperature is increased by about 11°C and the liquidus temperature is increased by about 32.31°C when the basicity is increased by 0.1 on average; the soft melting range is 16 to 24°C.

## 4 Conclusions

- 1. According to the simulation calculation of Factsage7.1 thermodynamic software, when the basicity is between 1.6 and 2.4, the mixed slag will precipitate solid solution,  $\alpha'$ -C<sub>2</sub>S, C<sub>2</sub>AS, C<sub>2</sub>SP and C<sub>2</sub>AF during the slow cooling process at 1,600°C. When the basicity is lower than 2.0, magnesium rose pyroxene (Ca<sub>3</sub>MgSi<sub>2</sub>O<sub>8</sub>) precipitates from the phase.
- 2. The melting mixed slag of blast furnace slag and steel slag (R = 1.6-2.4) was calcined at 1,450°C for 1 h. With the increase of basicity, the content of gehlenite decreased from 62.56 to 30.28%, the content of spinel increased from 4.82 to 27.13%, and the content of calcium ferrite increased from 9.35 to 14.63%. When the basicity of mixed slag is 2.0, the proportion of  $C_2S$  formation is the highest, reaching 13.67%. Therefore, it is considered that controlling the slag basicity at about 2.0 is beneficial to

- reduce the content of the non-gelatinized mineral calcium alumino vellow feldspar and promote the generation of the gelatinized mineral C<sub>2</sub>S.
- 3. With the increase of basicity, the content of  $Al_2O_3$  in the molten slag of blast furnace slag and steelmaking slag decreases, the content of low melting point calcium aluminum melilite generated decreases, and the melting temperature of the mixed slag increases continuously. The basicity is between 1.6 and 2.0. The hemispherical temperature increases by about 11°C and the melting range is between 16 and 24°C, when the basicity increases by 0.1. When the basicity is higher than 2.0, the melting temperature of the mixed slag rises sharply.

Acknowledgments: The project was supported by the National Key R&D Program Grant (2020YFC1909105) and the Inner Mongolia Autonomous Region Science and Technology Major Project (2021ZD0016-05-04).

Funding information: National Key R&D Program funded project (2020YFC1909105); Inner Mongolia Autonomous Region Science and Technology Major Special Project (2021ZD0016-05-04).

Author contributions: Shuai Hao: the experimental results are analyzed and a paper is written. Guo-ping Luo: The theory of the paper is guided, and the relevant content of the article has been modified. Yin-sheng Chen: provide experimental data and assist in analysis. Sheng-li An: valuable suggestions are given for experimental research. Yi-fan Chai and Wei Song: guided the whole experiment process.

Conflict of interest: No conflict of interest exits in the submission of this manuscript, and the manuscript is approved by all authors for publication.

Data availability statement: All authors can confirm that all data used in this article can be published in the Journal "High Temperature Materials and Processes."

## References

- [1] Xie, T. and L. S. Taylor. Feasibility study on self-pulverization of converter Slag. Journal of Anhui University of Technology (Natural Science Edition), Vol. 33, No. 2, 2016, pp. 105-109.
- Deng, Z. H., J. Wang, and Y. Zhou. Study on mineral facies of converter slag. Journal of Anhui University of Technology (Natural Science Edition), Vol. 28, No. 3, 2011, pp. 201-204.

- Lin, C. Basic research on self-pulverization and Vanadium extraction from steelmaking slag of stone coal converter. Master's Thesis. Anhui University of Technology, China,
- [4] Zhang, Y. Z. and Y. B. Lei. Analysis of mineral phase composition and Micromorphology of Steelmaking slag. Metallurgical Analysis, Vol. 31, No. 9, 2011, pp. 11-17.
- Feng, S. K., C. J. Liu, and M. F. Jiang. Analysis of phase composition of chromium bearing steelmaking slag under different cooling conditions. Proceedings of the 18th (2014) National Steelmaking Academic Conference -S09: Environmental Protection, 2014-48-52.
- Zhu, G. H., Y. S. Qian, and L. G. Jin. Volume stability of steelmaking slag and development and utilization of modified steelmaking slag powder. China Cement, 2022, No. 3, pp. 85-89.
- Zhao, H. Study on aging treatment and properties of road steelmaking slag. Western Transportation Science and Technology, 2021, No. 4, pp. 91-94.
- Zou, H. N. and Y. Feng. Analysis of soaking aging treatment time of steelmaking slag. Comprehensive Utilization of Fly Ash, 2016, No. 1, pp. 26-28.
- Qin, L. Q. Effect of aging on volume and water stability of steelmaking slag and asphalt concrete. Sino-Foreign Highway, 2019, Vol. 39, No. 6, pp. 273-279.
- Zou, M., Y. Shen, and J. Liu. Review on application of steelmaking slag powder in cement-based materials. Bulletin of the Chinese Ceramic Society, 2021, Vol. 40, No. 9, pp. 2964-2977.
- Guo, J. L., J. X. Zhao, and M. Huang. Review and suggestion of comprehensive utilization technology of steelmaking slag. China Metallurgy, Vol. 19, No. 2, 2009, pp. 35-38.
- [12] Li, Y. Study on preparation of solid waste based cementing materials and concrete with handan iron and steel metallurgical slag. Doctoral Thesis. University of Science and Technology Beijing, China, 2021.
- [13] Wang, Z. Y. and M. Wang. Research progress of dicalcium silicate and its Main mineral low calcium cement. Materials Review, Vol. 30, No. 1, 2016, pp. 73-78.
- [14] Fan, Z. M. Experimental study of steelmaking slag powder as cement mixture. China Cement, Vol. 1, 2022, pp. 92-94.
- [15] Wang, Z. Research on steelmaking slag as cement mixture, Hebei University of Engineering, Handan, 2020.
- Gencel, O., O. Karadag, O. H. Oren, and T. Bilir. Steelmaking slag and its applications in cement and concrete technology: A review. Construction and Building Materials, Vol. 283, 2021, id. 122783.
- [17] Xu, Y., Q. L. Wang, C. G. Hu, and Z. Z. Zhang Study on preparation of High Activity and High stability Steelmaking slag. Comprehensive Utilization of Mineral Resources, Vol. 4, 2019, pp. 106-110.
- [18] Deng, Z. H., J. Wang, H. C. Wang, Y. Zhou, B. G. Wu, and Y. C. Dong. Effect of P2O5 on mineral structure of converter Steelmaking slag. Journal of Anhui University of Technology (Natural Science Edition), Vol. 31, No. 4, 2014,
- [19] Zhang, Z. L. and R. Chen. Phase composition and microstructure of converter steelmaking slag. Journal of Materials and Metallurgy, Vol. 18, No. 1, 2019, pp. 37-40.

- [20] Xiao, Y. L., Y. D. Li, J. Y. Xiang, X. W. Lv, and H. L. Wang. Effect of cooling rate on phase structure and stability of steelmaking slag. *Steel Making*, Vol. 37, No. 6, pp. 76–81.
- [21] Rao, L. Study on internal law of composition, structure and properties of converter steelmaking slag and its application. Doctoral Thesis. University of Science and Technology Beijing, China, Beijing, 2020.
- [22] Zhang, Z. S., F. Lian, H. Q. Liao, Q. Yang, and W. B. Cao. Properties of steelmaking slag modified by iron tailings at high temperature. *Journal of University of Science and Technology Beijing*, Vol. 34, 2012, pp. 1379–1384.
- [23] Liu, S. Y., Z. J. Wang, B. Peng, C. S. Yue, M. Guo, and M. Zhang. Physical and chemical basis of steelmaking slag modified by blast furnace slag. *Journal of Engineering Science*, Vol. 40, 2018, pp. 557–564.
- [24] Xiang, R. H. Study on preparation and foaming modification of reconstituted steelmaking slag powder with medium and high activity. Master's Thesis. Guilin University of Technology, China, 2021.
- [25] Wang, H. G., B. Peng, C. S. Yue, L. Wu, G. B. Qiu, and Z. T. Bai. Research progress and prospect of steel slag modification.

- *Environmental Engineering*, Vol. 38, No. 5, 2020, pp. 133–137, 106.
- [26] Lei, Y. B., Y. Z. Zhang, H. W. Xing, Y. Long, and T. L. Tian. High temperature Melting and digestion of free CaO from converter slag mixed with fly ash. *Hebei Metallurgy*, Vol. 4, 2011, pp. 11–14.
- [27] Li, Z., S. Zhao, X. Zhao, and T. He. Cementitious property modification of basic oxygen furnace steelmaking slag. *Construction and Building Materials*, Vol. 48, 2013, pp. 575–579.
- [28] Zhang, X. Carbonation mechanism of steelmaking slag products modified by zeolite. Master's Thesis. Dalian University of Technology, China, 2021.
- [29] Liu, Z., Y. C. Wang, F. G. Zhao, G. P. Luo, and B. Zhao. Influence of binary basicity on physical properties of blast furnace slag of Baogang Group. *Journal of Iron and Steel Research*, Vol. 31, No. 8, 2019, pp. 696–701.
- [30] G. L. Zhao, D. Q. Cang, and Y. H. Lin. Preparation of high acidity coefficient mineral wool by modified molten steelmaking slag. *Journal of Iron and Steel Research*, 2022, Vol. 34, No. 2, pp. 142–149.